Pergamon

*Phys. Chem. Earth (B)*, Vol. 25, No. 10–12, pp. 1237–1242, 2000

1464-1909/00/$ - see front matter

PII: S1464-1909(00)00186-6

# Assimilation of Radar Data in Mesoscale Models: Physical Initialization and Latent Heat Nudging

**G. Haase[1], S. Crewell[1], C. Simmer[1] and W. Wergen[2]**

[1]Meteorological Institute, University of Bonn, Bonn, Germany
[2]German Weather Service, Offenbach, Germany

*Received 16 June 2000; accepted 7 July 2000*

**Abstract.** The increasing availability of quality controlled remotely sensed data (e.g. products from weather radar networks) as well as enhanced computer capacity allows an efficient use of these data in numerical weather prediction (NWP) models. In this paper two different assimilation techniques for radar measurements in mesoscale models are presented: a physical initialization (PI), currently under development at the University of Bonn, and a latent heat nudging (LHN) method implemented at the German Weather Service (DWD). Both algorithms are designed for the non-hydrostatic limited-area model LM (Lokal-Modell) of DWD. Input data are standard DWD measurements: national radar composites (reflectivities) and synoptical observations (temperature and dew point). Within the PI scheme the LM profiles of vertical wind, specific water vapor, and cloud water content are adjusted in such a way, that the model reproduces the radar derived precipitation. In the LHN scheme the prognostic variables temperature and specific humidity are changed. In PI and LHN runs with synthetic radar data the life-cycle of a single convective storm was well represented.


## 1 Introduction

Numerical prediction of precipitation strongly depends on the accurate representation of the initial state of the atmosphere and the parameterization of precipitation in the model. An error in the initial state can amplify through the modelling process and result in drastic variations of the predicted precipitation fields. Typically NWP model runs are initialized in a dry state and several hours pass until the hydrological cycle is established (spin-up time). A model consistent assimilation of precipitation reduces this time significantly and makes nowcasting possible. Furthermore, the forecast of surface pressure, precipitation, and dynamics will be improved.

There are two basic approaches for data assimilation: *sequential* or *real-time assimilation*, which only considers observations made in the past until the time of analysis, and *non-sequential* or *retrospective assimilation*, where observations from the future can be used, e.g. in a reanalysis exercise. Another distinction can be made between methods that are *intermittent* or *continuous* in time, whereas the latter is physically more realistic. Compromises between these approaches are possible.

Various techniques for assimilating precipitation data in NWP models have been developed. They differ in their numerical costs, their suitability for real-time data assimilation, and the model variables adjusted.

In three-dimensional variational data assimilation methods all relevant meteorological fields are modified simultaneously at every observation time. Afterwards, the forecast is continued on the basis of the modified fields. The UK Met.Office has developed such a technique for operational use (Barker, 1996). Detailed information about the three-dimensional variational data assimilation method was published by Courtier et al. (1998), Rabier et al. (1998), and Andersson et al. (1998).

Zupanski and Mesinger (1995) proposed a four-dimensional variational data assimilation (4DVAR) technique for precipitation data. Its basic idea is to minimize the difference between time series of objective analyses and model forecasts variational over a finite time period (Daley, 1991) considering the error characteristics of the observations and the model (Treadon, 1996). Disadvantages of 4DVAR are its great computional costs and the complex inversion of the nonlinear processes (e.g. the parameterization of precipitation) in an adjoint model.

The physical initialization, first mentioned by Krishnamurti et al. (1984), is similar to continuous data assimilation providing the information to the model every timestep. The PI method focuses on consistent model

*Correspondence to:* G. Haase, Meteorological Institute, University of Bonn, Auf dem Hügel 20, D-53121 Bonn, Germany, email: ghaase@uni-bonn.de

physics, which can generate the assimilated precipitation data. The similarity algorithm, the cumulus parameterization, and the algorithm, which restructures the vertical distribution of humidity, were inverted (Krishnamurti and Bedi, 1996). During the pre-forecast nudging phase the moisture and wind fields are modified by assimilating satellite-derived rain rates and outgoing longwave radiation (Krishnamurti et al., 1993).

A fourth approach of assimilating precipitation is the latent heat nudging, where increments of moisture and temperature are added throughout the pre-forecast period (Jones and Macpherson, 1997). Manobianco et al. (1994) applied this technique to an extratropical cyclone by using satellite derived precipitation. They found an improved forecast of the cyclones position even when the rain rate is not correct.

For the non-hydrostatic limited-area model LM (Lokal-Modell), which is the current operational NWP model of the DWD, precipitation assimilation is approached in two different ways. A latent heat nudging (LHN) technique, mostly comparable to the method presented by Jones and Macpherson (1997), was recently implemented. The physical initialization (PI) scheme, currently under development at the University of Bonn, is based on the ideas of Krishnamurti et al. (1984). It is particularly designed for non-hydrostatic models (vertical wind nudging) and extratropical areas. In contrast to Krishnamurti et al. (1984) our scheme utilizes radar instead of satellite data as input.

This paper is organized as follows: Section 2 gives a brief summary of the LM. The input data for the PI and the LHN method are summarized in sect. 3. In sects. 4 and 5 both assimilation techniques are explained in detail. Simulation results for a sensitivity study for July 13, 1999 are presented in sect. 6.

## 2 Lokal-Modell

The LM (Doms and Schättler, 1999), which is part of the new NWP system of the DWD, started routine operation on December 1st, 1999 with a horizontal resolution of 7 km. In the simulations presented in this paper the model (version 1.27) was run with 2.8 km horizontal resolution for an area of approximately 400 km × 400 km in the northern part of Germany (Fig.1).

The initial and boundary fields for the LM forecast are provided by the Deutschlandmodell, which is a hydrostatic mesoscale model with 14 km gridsize and 30 vertical levels. The LM has a generalized terrain-following sigma coordinate, which divides the atmosphere into 35 levels. The prognostic model variables calculated on an Arakawa-C-grid are the wind vector, temperature, pressure, specific water vapor, and cloud water content. Rain and snow flux are diagnostic variables. The integration timestep is 30 seconds. The model includes a grid-scale cloud and precipitation scheme as well as a parameterization of moist convection (Tiedtke mass flux scheme). However, for this study the convection parameterization was switched off, because it was assumed that convection will be resolved by model resolution. Further characteristics of the LM are a level-2 turbulence parameterization, a delta-2-stream radiation transfer scheme, and a 2-layer soil model.

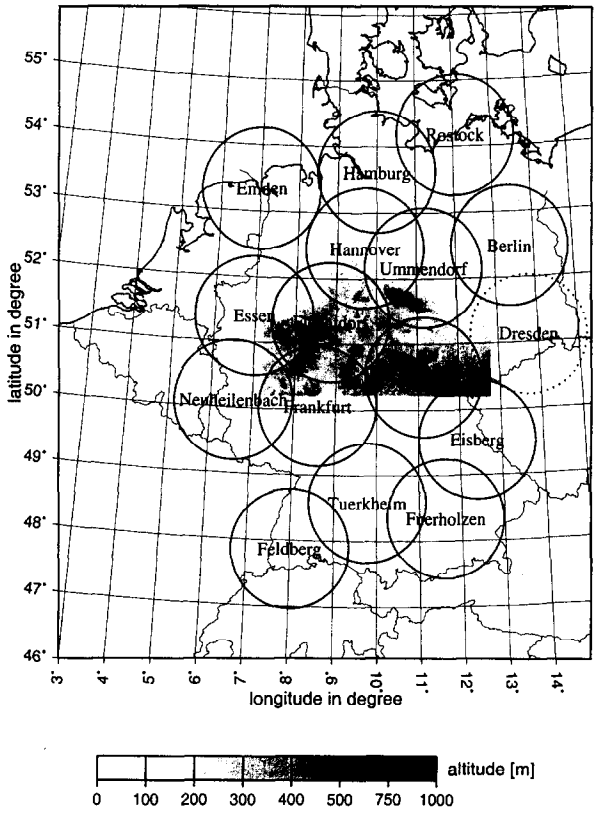


**Fig. 1.** DWD radar network and orography of the LM domain. The circles marking each radar site have a radius of 100 km.

## 3 Input Data

Both assimilation techniques, physical initialization and latent heat nudging, use DWD standard observations as input.

- **national radar composite**
  The two-dimensional product with a horizontal resolution of 4 km is provided operationally by the DWD radar network every 15 minutes and contains six reflectivity classes. The mean reflectivity of each class ($Z_{OBS}$ in $mm^6/m^3$) is converted into a rain rate ($RR'_{OBS}$ in mm/h) following the Z–R relation for the DWD radar network (Schreiber, 1997)

$$RR'_{OBS} = \left(\frac{Z_{OBS}}{256}\right)^{1/1.42} . \quad (1)$$

The rain rate is converted into a precipitation flux ($RR_{OBS}$ in kg/m$^2$s).

- **synoptic ground observations**
  Temperature ($T_{OBS}$ in K) and dew point ($\tau_{OBS}$ in K) in 2m height are measured at the DWD synoptic ground stations at least four times a day. The mean distance between the stations is about 30 km. The lifting condensation level ($LCL$ in m) is calculated according to

$$LCL = 121\,(T_{OBS} - \tau_{OBS})\ . \tag{2}$$

Within the data pre-processing, rain rates and lifting condensation levels are interpolated linearly in time and space to LM timestep and resolution.

The error characteristics of the precipitation estimates are also relevant. Several sensitivity studies, in which errors were deliberately introduced into the precipitation data found, that positional errors led to a significantly reduced forecast improvement. In contrast, rate errors degraded the forecast to a lesser degree (Manobianco et al., 1994). Therefore, the crude resolution of the observed radar reflectivities (only six classes) is not a serious problem.

## 4 Physical initialization

Within the PI scheme the model and boundary fields of vertical wind ($w$ in m/s), specific water vapor ($q_v$ in kg/kg), and cloud water content ($q_c$ in kg/kg) are modified (Tab.1). Currently, the cloud top height ($z_{ct}$ in m) at model gridpoints with observed precipitation is temporally and spatially constant. A more accurate value can be derived from three-dimensional radar products, where the maximum echo heights are assumed to be a first guess for the cloud top height. Satellite and radiosonde data may contribute additional information. The cloud base height ($z_{cb}$ in m) is set to the $LCL$ derived from synoptic observations according Eq.(2). In the PI scheme the $LCL$ is used instead of the observed cloud base height, because many synoptic ground stations do not measure this parameter at night.

The vertical wind inside a cloud, defined by $z_{ct}$ and $z_{cb}$, is derived assuming a simplified precipitation mechanism. This mechanism is based on the continuity equations for the partial densities of saturated water vapor ($\rho_v^\star$ in kg/m$^3$) and precipitable water ($\rho_l$ in kg/m$^3$):

$$\partial\rho_v^\star/\partial t = -\nabla(\rho_v^\star \mathbf{v}) - K \tag{3}$$

$$\partial\rho_l/\partial t = -\nabla(\rho_l \mathbf{v_l}) + K\ , \tag{4}$$

where $\mathbf{v}$ and $\mathbf{v_l}$ are the three-dimensional air and water velocity vectors and $K$ is the conversion term due to condensation and evaporation. Adding both equations and splitting each term into a horizontal and a vertical part (stationarity assumed) leads to:

$$\nabla_\mathbf{h}(\rho_v^\star \mathbf{v_h}) + \frac{\partial(\rho_v^\star w)}{\partial z} + \nabla_\mathbf{h}(\rho_l \mathbf{v_{h,l}}) + \frac{\partial(\rho_l w_l)}{\partial z} = 0\ , \tag{5}$$

**Table 1.** LM variables modified within the PI scheme ($z_{surf}$: height of surface topography, $rh$: relative humidity, $q_v^\star$: saturation specific humidity)

| height interval | $RR_{OBS} > 0$ | $RR_{OBS} < 0$ |
|---|---|---|
| $z > z_{ct}$ | $w = 0$<br>$rh_{max} = 75$<br>$q_c = 0$ | $w = 0$<br>$q_v = q_{v,MOD}$<br>$q_c = 0$ |
| $z_{ct} \geq z \geq z_{cb}$ | $w = w(z, RR_{OBS})$<br>$q_v = q^\star_{v,MOD}$<br>$q_c = q_c(z, T_{MOD}, q_{v,MOD})$ | $w = 0$<br>$q_v = q_{v,MOD}$<br>$q_c = 0$ |
| $z < z_{cb}$ | $w = w(z_{cb})\ \frac{z - z_{surf}}{z_{cb} - z_{surf}}$<br>$q_v = q^\star_{v,MOD}(z_{cb})$<br>$q_c = 0$ | $w = 0$<br>$q_v = q_{v,MOD}$<br>$q_c = 0$ |

where $\rho_l w_l$ is the precipitation flux ($RR$ in kg/m$^2$s). Note that $RR$ has the same sign as the vertical wind. Neglecting the horizontal transport of precipitable water leads to:

$$\nabla_\mathbf{h}(\rho_v^\star \mathbf{v_h}) + \frac{\partial(\rho_v^\star w)}{\partial z} = -\frac{\partial RR}{\partial z}\ . \tag{6}$$

The precipitation flux at the surface is derived from radar observations according Eq.(1). At present, the profile of the precipitation flux has a very simple form: beneath the cloud base evaporation is neglected and inside the cloud the precipitation flux decreases linearly from the cloud base to the cloud top:

$$RR(z) = RR(z_{cb})\ \frac{z_{ct} - z}{z_{ct} - z_{cb}} \tag{7}$$

It is also assumed that the vertical wind at the cloud top vanishes. In order to derive an equation for the vertical wind, the structure of the horizontal divergence of saturated water vapor in Eq.(6) has to be approximated. A sinusoidal profile accomplishes all requirements:

$$\nabla_\mathbf{h}(\rho_v^\star \mathbf{v_h}) = \tilde{c}\ \sin\left(\frac{\pi}{2}\,\frac{z - z_{cb}}{z_{ct} - z_{cb}}\right) \tag{8}$$

with

$$\tilde{c} = \frac{RR(z_{cb})}{z_{ct} - z_{zb}}\ \frac{\pi}{2}\ \left(1 + \frac{\rho_v^\star(z_{cb}) w(z_{cb})}{RR(z_{cb})}\right)\ . \tag{9}$$

The horizontal divergence of saturated water vapor vanishes at the cloud base and becomes maximal at the cloud top. Inserting (7) and (9) in (6) leads to:

$$\frac{\partial(\rho_v^\star w)}{\partial z} = \frac{RR(z_{cb})}{z_{ct} - z_{zb}}\left[1 - \frac{\pi}{2}\left(1 + \frac{\rho_v^\star(z_{cb}) w(z_{cb})}{RR(z_{cb})}\right) \sin\left(\frac{\pi}{2}\,\frac{z - z_{cb}}{z_{ct} - z_{cb}}\right)\right]\ . \tag{10}$$

After discretization of Eq.(10) an expression for the vertical wind inside the cloud at model level $k$ can be derived:

$$w_k = \left(\rho^\star_{v,k}\right)^{-1}\left\{\rho^\star_{v,k-1} w_{k-1} - (z_{k-1} - z_k)\frac{RR(z_{cb})}{z_{ct} - z_{zb}} \left[1 - \frac{\pi}{2}\,(1 + c)\sin\left(\frac{\pi}{2}\,\frac{z_{k-1/2} - z_{cb}}{z_{ct} - z_{cb}}\right)\right]\right\}\ . \tag{11}$$

The term

$$c = \frac{\rho_v^*(z_{cb})w(z_{cb})}{RR(z_{cb})} \tag{12}$$

in Eq.(11) expresses the ratio between the vertical fluxes of saturated water vapor and liquid water at the cloud base. Its value characterizes the shape of the vertical wind profile. In all the following simulations $c$ is set to 0.5 matching a mean observed $w$ profile for raining clouds. The parameter $c$ is the only tuning parameter in the simplified precipitation mechanism.

The vertical wind outside the cloud is approximated as follows: above the cloud the vertical wind is set to zero and beneath the cloud a linear gradient is assumed (Tab.1).

The maximum relative humidity ($rh_{max}$) above $z_{ct}$ is fixed to 75%. Inside the cloud saturation is assumed. Below the cloud base the specific humidity is equal to the saturation specific humidiy at the cloud base.

The specific cloud water content above and beneath the cloud is assumed to be zero. If the temperature inside the cloud is less than 253.16 K the adiabatic liquid water content $q_{c,ad}$ is calculated according to Hargens (1993):

$$q_{c,ad}(z) = \int_{z_{cb}}^{z} \rho_{air}(z')\frac{c_p}{L}(\Gamma_d - \Gamma_s)dz' \ , \tag{13}$$

where $\rho_{air}$ is the density of air, $c_p$ is the specific heat at constant pressure, $L$ is the latent heat of vaporization, $\Gamma_d$ is the dry adiabatic and $\Gamma_s$ is the pseudoadiabatic lapse rate. Observations have shown that clouds exist mostly of super-cooled water at temperatures above 253.15 K (Rogers and Yau, 1989). Moreover, the LM version used in this study contains no ice scheme. The reduction of the liquid water content by entrainment of unsaturated air, precipitation formation, and freezing is considered by Warner (1955):

$$q_c(z) = q_{c,ad}\,[-0.145\,\ln(z - z_{cb}) + 1.239] \ . \tag{14}$$

Eq.(14) provides the modified specific cloud water contents for the PI scheme.

At gridpoints without observed precipitation the vertical wind and the specific cloud water content are set to zero, the specific water vapor content remains unchanged.

## 5 Latent heat nudging

The LHN technique implemented at the DWD for the LM is briefly described in this section. More details can be found in Jones and Macpherson (1997).

Radar derived and model rain rates ($RR_{OBS}$ and $RR_{MOD}$) are blended at each timestep:

$$RR = \alpha \cdot RR_{OBS} + (1 - \alpha) \cdot RR_{MOD} \ . \tag{15}$$

The weighting factor $\alpha$ is a function of temporal and spatial distance to the radar observation. For large distances $\alpha$ is small and the weight of the observation is reduced. This is a simple estimation of errors in the radar rain rates.

The model profiles of latent heat release ($\Delta T_{LH,MOD}$) are scaled as follows:

$$c_p\,\Delta T_{LH} = \frac{RR}{RR_{MOD}}\,c_p\,\Delta T_{LH,MOD} \ . \tag{16}$$

If $RR_{OBS} = 0$ and $RR_{MOD} > 0$ model latent heating is suppressed. If $RR_{OBS} > 0$ and $RR_{MOD} = 0$ the scheme is searching for a nearby gridpoint with $RR_{MOD} \sim RR_{OBS}$. Otherwise a "climatological" profile is selected.

The numerical noise is controlled by vertical (horizontal) filtering of the heating profiles (increments). Upscaling and downscaling are limited due to absolute limits for the increments.

The LHN scheme includes also a humidity adjustment. If the heating is reduced, $q_v$ is decreased in order to maintain $rh$. Otherwise $q_v$ is increased to reach 100% relative humidity over the nudging timescale.

## 6 Sensitivity study

Three LM forecasts are performed for July 13, 1999: a control run (without any changes in the model code), a run with PI, and one with LHN (all initialized at 12 UTC). For a better understanding of the results, a temporally and spatially fixed precipitation pattern is assimilated specified for a real atmospheric state of a convective situation. The artificial precipitation area with an extension of approximately 950 km$^2$ (Fig.2) is located in the south-eastern part of the model domain. Its maximum rain rate is 15 mm/h.

The forcing period is one hour for the LHN and 15 minutes for the PI run with a one hour free LM run afterwards. As already mentioned, the LHN method uses a nudging term in the thermodynamic equation, while in the PI scheme the LM profiles of $w$, $q_v$, and $q_c$ are replaced by modified ones at the beginning of each timestep in the assimilation period. Note that in the PI scheme the vertical wind and humidity forcing is fixed during this time. A more consistent nudging method for the PI will be implemented soon. Then the forcing period of the PI and the LHN run will be equal (one hour). The tuning parameter $c$ in Eq.(12) is 0.5 as mentioned above. In the PI run the specific cloud water content inside the artificial precipitation area is not modified. The cloud top height is 4000 m, whereas the cloud base is set to the $LCL$ derived from synoptic ground observations.

In the control run (not shown) only single precipitation cells of low intensity are simulated one hour after initialization and the vertical wind field has no characteristic structures. The results of the PI and LHN runs

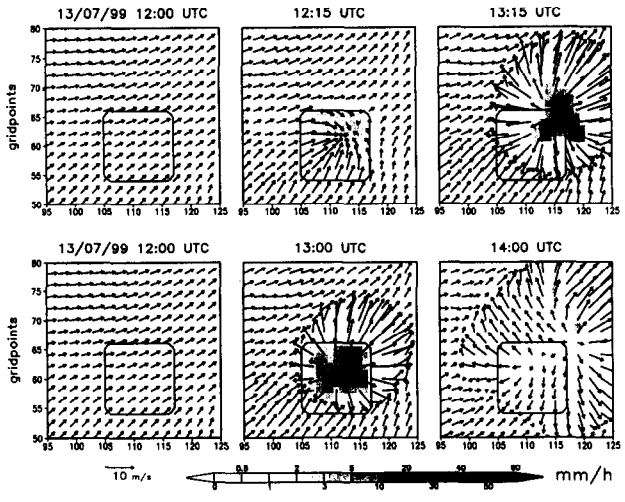


**Fig. 2.** Horizontal sections of precipitation rate (gray shaded) and near surface wind (barbs in z=100 m) for the PI (upper panel) and the LHN run (lower panel). Note that the time intervals are different. The square indicates the location of the artificial precipitation area.

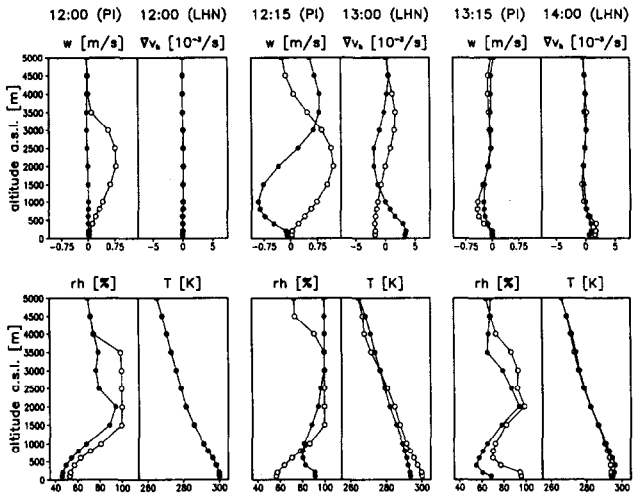


**Fig. 3.** Profiles of vertical wind ($w$), temperature ($T$), relative humidity ($rh$), and horizontal wind divergence ($\nabla \mathbf{v_h}$) at gridpoint (111,60) for the PI (open circles) and the LHN run (close circles). Note that the time intervals are different.

at the beginning/end of the assimilation period and after one hour free LM run are shown in Fig.2 and 3. It has to be noted that the time intervals are different, because the forcing period in the LHN run is longer than in the PI run.

The thermal forcing (LHN) and the modification of $w$, $q_v$, and $q_c$ (PI) in its current implementation, result in comparable influence on vertical velocity and flow patterns. In the presented case, the evaporation of precipitation in a dry boundary layer below the cloud base creates strong downdrafts and low level divergence. In the LHN run this already happens during the one hour forcing period, while in the PI run, due to the prescribed $w$ profiles, this occurs in the one hour free LM run (Fig.3). There is no precipitation simulated at the initialization time (12 UTC) due to a lack of cloud water in the LM analysis. The slight temperature differences at 12:15 UTC (PI) / 13:00 UTC (LHN) shown in Fig.3 are mainly caused by different times of model output. For a better understanding of the differences between both runs, the temporal resolution of model output are to be adapted.

## 7 Summary and discussion

In order to incorporate radar derived precipitation data into the LM, the present study developed an assimilation method executing physical initialization. Afterwards, a simple nudging of vertical wind, specific water vapor, and cloud water content was conducted. Another assimilation approach is the latent heat nudging implemented at the DWD and similar to the method developed by Jones and Macpherson (1997).

The effects of both assimilation techniques on the forecast for July 13, 1999 were shown. For a better comparison of the results, a temporally and spatially fixed rainfall area was assimilated. In both LM runs (PI and LHN) the life-cycle of a single convective storm was well represented. The flow and precipitation patterns/amounts were almost identical. The life-time of the artificial cell was less than two hours, which is comparable to observations.

On the basis of this sensitivity study it is not possible to determine whether the spin-up time and the position error of the precipitation forecast are reduced or not. Therefore, assimilation runs with real radar data has to be conducted.

Moreover, the LM simulation was not long enough to perform statistical investigations. Comparing forecasted and measured precipitation by means of objective skill scores offers the opportunity to easily assess the quality of the weather forecast model (Jones and Macpherson, 1997). When the radar measurement is converted into a rain rate, conventionally by a simple Z-R relation, the propagation of the radar beam in the three-dimensional space as well as the effects of attenuation by hydrometeors and atmospheric gases are neglected. The direct comparison of radar reflectivities, measured and forecasted, reduces some of the uncertainties pertinent to the comparison of modelled to radar derived precipitation. This can be done with the radar simulation model, RSM, (Haase and Crewell, 2000). The RSM is able to simulate radar reflectivities of any kind of radar situated within the LM domain, and hence allows a quick quality control of the predicted hydrometeor components.

Further sensitivity studies have shown that the PI is more suitable for nowcasting convective than frontal events (Gross et al., 2000). For stratiform precipitation events compensating downdrafts are to be considered. Additional information about the cloud top height as

well as the vertical structure of the radar derived rain rate will have a positive effect on the assimilation of precipitation.

Despite the above mentioned problems, the results of the present study are encouraging. Additional benefits of both assimilation approaches are low computional costs and the fact that solely operationally measured data are used.

*Acknowledgements.* This work has been funded by the Research Department of the German Weather Service (DWD). The latent heat nudging was implemented in the LM by Christina Köpken. We thank Patrick Gross, Christina Köpken and both reviewers for the helpful discussions and comments.

## References

Andersson, E., Haseler, J., Undén, P., Courtier, P., Kelly, G., Vasiljević, D., Branković, C., Cardinali, C., Gaffard, C., Hollingsworth, A., Jakob, C., Janssen, P., Klinker, E., Lanzinger, A., Miller, M., Rabier, F., Simmons, A., Strauss, B., Thépaut, J.-N., and Viterbo, P., The ECMWF implementation of three-dimensional variational assimilation (3D-Var). III: Experimental results, *Quarterly Journal of the Royal Meteorological Society*, *124*, 1831–1860, 1998.

Barker, D. M., Progress report on the development of a variational data assimilation scheme at the UK Met. Office, in *Preprints, 11th AMS NWP Conference, Norfolk, Virginia, USA*, pp. 229–231, 1996.

Courtier, P., Andersson, E., Heckley, W., Pailleux, J., Vasiljević, D., Hamrud, M., Hollingsworth, A., Rabier, F., and Fisher, M., The ECMWF implementation of three-dimensional variational assimilation (3D-Var). II: Formulation, *Quarterly Journal of the Royal Meteorological Society*, *124*, 1783–1807, 1998.

Daley, R., *Atmospheric data analysis*, Cambridge University Press, 1991.

Doms, G. and Schättler, U., *The nonhydrostatic limited-area model LM (Lokal-Modell) of DWD – part I: scientific documentation*, German Weather Service (DWD), Research Department, P.O. 100465, D-63004 Offenbach, 1999.

Gross, P., Simmer, C., Müller, G., and Haase, G., Use of remote sensing for validation and assimilation in mesoscale models, in *Remote sensing and hydrology 2000*, IAHS Red Book, accepted, 2000.

Haase, G. and Crewell, S., Simulation of radar reflectivities using a mesoscale weather forecast model, *Water Resources Research*, accepted, 2000.

Hargens, U., *Fernerkundung des Flüssigwassergehaltes von Wolken*, Ph.D. thesis, Institut für Meereskunde, Christian-Albrechts-Universität Kiel, 1993.

Jones, C. D. and Macpherson, B., A latent heat nudging scheme for the assimilation of precipitation data into an operational mesoscale model, *Meteorological Applications*, *4*, 269–277, 1997.

Krishnamurti, T. N. and Bedi, H. S., A brief review of physical initialization, *Meteorology and Atmospheric Physics*, *60*, 137–142, 1996.

Krishnamurti, T. N., Ingles, K., Cocke, S., Kitade, T., and Pasch, R., Details of low latitude medium range numerical weather prediction using a global spectral model, part ii: effects of orography and physical initialization, *Journal of the Meteorological Society of Japan*, *62*, 613–649, 1984.

Krishnamurti, T. N., Bedi, H. S., and Ingles, K., Physical initialization using SSM/I rain rates, *Tellus*, *45*, 247–269, 1993.

Manobianco, J., Koch, S., Karyampudi, V. M., and Negri, A. J., The impact of assimilating satellite-derived precipitation rates on numerical simulations of the ERICA IOP 4 cyclone, *Monthly Weather Review*, *122*, 341–365, 1994.

Rabier, F., McNally, A., Andersson, E., Courtier, P., Undén, P., Eyre, J., Hollingsworth, A., and Bouttier, F., The ECMWF implementation of three-dimensional variational assimilation (3D-Var). II: Structure functions, *Quarterly Journal of the Royal Meteorological Society*, *124*, 1809–1829, 1998.

Rogers, R. R. and Yau, M. K., *A short course in cloud physics*, Pergamon Press, 1989.

Schreiber, K., *Der Radarverbund*, German Weather Service (DWD), Technical Infrastructure Department, P.O. 100465, D-63004 Offenbach, 1997.

Treadon, R. E., Physical initialization in the NMC global data assimilation system, *Meteorology and Atmospheric Physics*, *60*, 57–86, 1996.

Warner, J., The water content of cumuliform cloud, *Tellus*, *7*, 449–457, 1955.

Zupanski, D. and Mesinger, F., Four-dimensional variational assimilation of precipitation data, *Monthly Weather Review*, *123*, 1112–1127, 1995.